

University of Groningen

## Equilibrium Solubility of CO<sub>2</sub> in Aqueous Potassium Taurate Solutions

Kumar, P.S.; Hogendoorn, J.A.; Feron, P.H.M.; Versteeg, G.F.

*Published in:*  
Industrial & Engineering Chemistry Research

*DOI:*  
[10.1021/ie020601u](https://doi.org/10.1021/ie020601u)

**IMPORTANT NOTE: You are advised to consult the publisher's version (publisher's PDF) if you wish to cite from it. Please check the document version below.**

*Document Version*  
Publisher's PDF, also known as Version of record

*Publication date:*  
2003

[Link to publication in University of Groningen/UMCG research database](#)

*Citation for published version (APA):*

Kumar, P. S., Hogendoorn, J. A., Feron, P. H. M., & Versteeg, G. F. (2003). Equilibrium Solubility of CO<sub>2</sub> in Aqueous Potassium Taurate Solutions: Part 1. Crystallization in Carbon Dioxide Loaded Aqueous Salt Solutions of Amino Acids. *Industrial & Engineering Chemistry Research*, 42(12), 2841-2852.  
<https://doi.org/10.1021/ie020601u>

**Copyright**

Other than for strictly personal use, it is not permitted to download or to forward/distribute the text or part of it without the consent of the author(s) and/or copyright holder(s), unless the work is under an open content license (like Creative Commons).

**Take-down policy**

If you believe that this document breaches copyright please contact us providing details, and we will remove access to the work immediately and investigate your claim.

*Downloaded from the University of Groningen/UMCG research database (Pure): <http://www.rug.nl/research/portal>. For technical reasons the number of authors shown on this cover page is limited to 10 maximum.*

# Equilibrium Solubility of CO<sub>2</sub> in Aqueous Potassium Taurate Solutions: Part 2. Experimental VLE Data and Model

P. S. Kumar,<sup>†,‡</sup> J. A. Hogendoorn,<sup>†</sup> S. J. Timmer,<sup>†</sup> P. H. M. Feron,<sup>§</sup> and G. F. Versteeg<sup>\*,†</sup>

OOIP Group, Faculty of Chemical Technology, University of Twente, P.O. Box 217, 7500 AE Enschede, The Netherlands, and TNO Environment, Energy and Process Innovation, 7300 AH Apeldoorn, The Netherlands

The solubility of CO<sub>2</sub> in aqueous potassium taurate solutions was measured at 298 and 313 K. Crystallization of the protonated amine (one of the reaction products) was observed during the absorption of CO<sub>2</sub> in concentrated amino acid salt solutions. The influence of crystallization on the equilibrium CO<sub>2</sub> absorption capacity of the amino acid salt solution was investigated. The difference in the thermodynamic characteristics of the aqueous amino acid salt solution and aqueous alkanolamines is discussed using the Deshmukh–Mather model (Deshmukh, R. D.; Mather, A. E. *Chem. Eng. Sci.* **1981**, *36*, 355). Because of a limited change in the ionic strength of the solution in the range of the measured CO<sub>2</sub> loading, a simplified model similar to the one proposed by Kent and Eisenberg (Kent, R.; Eisenberg, B. *Hydrocarbon Process.* **1976**, *55*, 87) is used to interpret the solubility data. In addition, the equilibrium constant of the carbamate hydrolysis reaction was experimentally measured for monoethanolamine and the potassium salt of taurine at 298 K.

## 1. Introduction

Removal of acid gases, such as CO<sub>2</sub> and H<sub>2</sub>S, by absorption in reactive solvents is a vital mass-transfer operation in a number of industrial activities, including the processing of natural gas or refinery gas and the production of gas via coal gasification. Because of the increasingly stringent environmental regulations, absorption in reactive solvents is also used from the removal of CO<sub>2</sub> from effluent gas streams such as flue gases from power generation plants. The widely used chemical solvents in the bulk or selective removal of CO<sub>2</sub> are aqueous alkanolamine solutions and amine-promoted alkaline salt solutions.<sup>1</sup> Some of the practical problems associated with alkanolamines in acid-gas-treating processes are their high volatility (especially for primary amines such as monoethanolamine), leading to vaporization losses in the stripper and their degradation in COS- or oxygen-containing gas streams. Aqueous alkaline salt solutions of amino acids can provide a possible alternative for aqueous alkanolamines. The amino acids have primarily been used in the past in minor quantities as “rate promoters” in conventional gas-treating processes such as the hot carbonate process. However, a few commercial processes (such as Alkacid M and Alkacid dik from BASF) have used amino acid salt solutions exclusively for the selective removal of acid gases. The ionic nature of these liquids offers many advantages over alkanolamines such as negligible volatility (and, consequently, negligible loss of solvent in the stripper); better resistance to degradation, especially in oxygen-rich atmospheres; and low viscosity (resulting

in a lower pressure drop in solvent circulation). The surface tension of these liquids is comparable to that of water, which is of tremendous advantage for their use in some of the latest-generation gas–liquid contactors, such as membrane contactors. In membrane contactors, wetting of the microporous membranes by aqueous alkanolamines is a major technical bottleneck in their use for CO<sub>2</sub> removal.<sup>2</sup> Currently, there is renewed interest in the use of amino acids for acid gas treatment, especially in removal of CO<sub>2</sub> from gas streams that also contain oxygen, such as flue gas.

The design of gas–liquid contactors for CO<sub>2</sub> removal using aqueous alkaline salts of amino acids requires information about the vapor–liquid equilibrium (VLE), among other properties, of the CO<sub>2</sub>–aqueous amino acid salt system. Unlike aqueous alkanolamine–CO<sub>2</sub> systems, for which large amounts of experimental VLE data are available in the literature, the published data on CO<sub>2</sub>–aqueous amino acid salt systems are scarce. Recently, Hook<sup>3</sup> made a qualitative study on the CO<sub>2</sub> absorption rates and capacities of the aqueous alkaline salts of some sterically and nonsterically hindered amino acids and found them to be comparable to the rates and capacities of aqueous alkanolamines of a similar class. A unique phenomenon associated with certain amino acids is the crystallization of a reaction product during CO<sub>2</sub> absorption, especially at high CO<sub>2</sub> loading (moles of CO<sub>2</sub> per mole of amino acid salt) and amino acid salt concentrations.<sup>3,4</sup> Kumar et al.<sup>4</sup> gave a relationship between the critical CO<sub>2</sub> loading value at which crystallization of the reaction product occurred for potassium taurate solutions. However, the influence of such crystallization on the solubility of CO<sub>2</sub> in aqueous amino acid salt solutions is not known. Thus, a real need exists for experimental data on the equilibrium solubility of CO<sub>2</sub> in aqueous amino acid salt solutions to understand the behavior of these absorption liquids qualitatively as well as quantitatively. Fortu-

\* To whom correspondence should be addressed. Tel.: 0031-53-4894337. Fax: 0031-53-4894774. E-mail: g.f.versteeg@ct.utwente.nl.

<sup>†</sup> University of Twente.

<sup>‡</sup> Presently at Shell Global Solutions International BV, P.O. Box 541, 2501 CM, The Hague, The Netherlands.

<sup>§</sup> TNO Environment, Energy and Process Innovation.



water,  $a_w$ , was set equal to its mole fraction.<sup>5</sup> The equilibrium constant for reaction 2, which was left out of the reaction scheme, can be expressed in terms of the equilibrium constants of reactions 3–5

$$K_{ov} = \frac{K_{CO_2}}{K_{AmA}K_{carb}} \quad (13)$$

The chemical reactions in the liquid phase are accompanied by the vapor–liquid equilibria of CO<sub>2</sub> and water. The equilibrium vapor pressure of CO<sub>2</sub> in the gas phase was related to the liquid-phase concentration using the experimental (physical) solubility data obtained in an earlier study, which were described using the model of Weisenberger and Schumpe<sup>11</sup>

$$P_{CO_2} = RTm_{CO_2}[CO_2] \quad (14)$$

where

$$\log(m_{CO_2,w}/m_{CO_2}) = K_s C_s \quad (15)$$

Here,  $m_{CO_2,w}$  is the physical solubility of CO<sub>2</sub> in water;  $C_s$  is the molar amino acid salt concentration; and  $K_s$  is the Sechenov constant, which is defined in terms of ion-specific ( $h_i$ ) and gas-specific ( $h_G$ ) constants as

$$K_s = \Sigma(h_i + h_G)z_i \quad (16)$$

Here,  $z_i$  is the charge number of the ion. The numerical values of the temperature-independent ion-specific constants were obtained from the work of Kumar et al.,<sup>12</sup> and the value of temperature-dependent gas (CO<sub>2</sub>) specific constant was obtained from the work of Weisenberger and Schumpe.<sup>11</sup>

For water, the vapor–liquid equilibrium is given by

$$P_w = a_w P_w^{sat} \quad (17)$$

Because the amino acid salt present in the liquid phase is in ionic form, it was assumed to be nonvolatile. The gas-phase total pressure in the present work was approximately 100 kPa. Therefore, the nonideality in the gas phase was neglected. In addition to the above equations, the following mass conservation and charge balance equations were also used in the equilibrium model

Amine mass balance

$$[\text{RNH}_2]_0 = [\text{RNH}_2] + [\text{RNH}_3^+] + [\text{RNHCOO}^-] \quad (18)$$

CO<sub>2</sub> mass balance

$$\alpha_{CO_2}[\text{RNH}_2]_0 = [\text{CO}_2] + [\text{RNHCOO}^-] + [\text{HCO}_3^-] + [\text{CO}_3^{2-}] \quad (19)$$

The principle difference between the VLE models of aqueous alkanolamines and amino acid salts is mostly related to the charge of the ionic species present in the liquid phase. The following remarks apply for amino acid salt systems: (1) The deprotonated amino acid that reacts with CO<sub>2</sub> is an anion with a single negative charge. (2) The protonated amino acid is a zwitterion and was considered here to be electrically neutral, as

for molecular species. (3) The concentration of the cation of the amino acid salt (K<sup>+</sup>) is the same as the initial amino acid salt concentration ( $[\text{RNH}_2]_0$ ). (4) The carbamate anion of the amino acid salt has a charge of -2.

The above remarks were incorporated into the model, yielding the following charge balance equation

$$[\text{K}^+] + [\text{H}^+] = [\text{RNH}_2] + [\text{OH}^-] + [\text{HCO}_3^-] + 2[\text{RNHCOO}^-] + 2[\text{CO}_3^{2-}] \quad (20)$$

**2.3. Liquid-Phase Nonideality.** The above set of equations can be solved by neglecting the nonideality in the liquid phase (i.e., by setting the values of the activity coefficients in all equilibrium relations to 1) and force fitting the thus-obtained simplified model to the experimental data. In this procedure, the equilibrium constants of reactions 3 (carbamate hydrolysis reaction;  $K_{carb}$ ) and 4 (amine deprotonation reaction;  $K_{AmA}$ ) are used as fit parameters. The equilibrium constants obtained in this way are apparent constants. This is also the basic approach of the equilibrium model proposed by Kent and Eisenberg,<sup>13</sup> which was found to fit very well for single alkanolamine–acid gas systems in the range of CO<sub>2</sub> loadings between 0.2 and 0.7 mol of CO<sub>2</sub> per mole of amine.

A number of semiempirical excess Gibbs free energy or activity coefficient models for aqueous electrolyte systems that are valid for ionic strengths representative of those found in industrial applications are available in the literature. These models basically account for the nonidealities in the liquid phase by taking into account various short-range and long-range interactions between different ionic and molecular species present in the solution. The most relevant models from the point of view of simplicity and thermodynamic soundness are those based on the extended Debye–Hückel theory<sup>5</sup> and the electrolyte–NRTL theory.<sup>14,15</sup> For a single amine–acid gas system, the Deshmukh–Mather model was found to be thermodynamically rigorous as well as simple from a computational point of view,<sup>16</sup> and therefore, it will be considered here. The model, which was proposed originally by Guggenheim,<sup>17</sup> uses the following equation for the activity coefficient of a solute species

$$\ln \gamma_i = \frac{-2.303Az_i^2 I^{0.5}}{1 + BaI^{0.5}} + 2 \sum_{j \neq w} \beta_{ij} [j] \quad (21)$$

where the subscript  $i$  denotes the solute species of interest. This model takes into account the long-range electrostatic (first term of eq 21) and short-range van der Waals (second term of eq 21) forces. The long-range electrostatic forces are taken into account by the Debye–Hückel term, whereas the short-range forces are taken into account through the binary interactions (parameters,  $\beta_{ij}$ ) between different molecular and ionic solutes. The Debye–Hückel limiting slope,  $A$ , and the parameter  $B$  are related to the dielectric constant of the solvent (water) according to the following relations<sup>18</sup>

$$A = 1.825 \times 10^6 (\epsilon T)^{-3/2} \quad (22)$$

$$B = 50.3 (\epsilon T)^{-1/2} \quad (23)$$

Although the parameter  $a$  in eq 21 is an adjustable parameter with units of angstroms, a constant value of

**Table 1. Literature Sources for the Various Equilibrium Constants Used in the VLE Model**

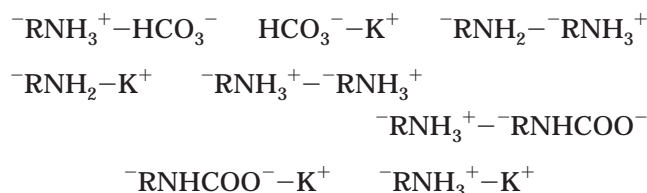
constant	temperature range (K)	ref
$K_w$	273–498	Tsonopoulos et al. <sup>19</sup>
$K_{CO_2}$	273–498	Edwards et al. <sup>20</sup>
$K_{HCO_3}$	273–498	Edwards et al. <sup>20</sup>
$K_{AmA}$	283–323	Perrin <sup>7</sup>

3 (as proposed by Guggenheim<sup>17</sup>) was used in the present work for all ionic species. Any associated errors resulting from this assumption are automatically taken into account during fitting of the binary interaction parameters. The ionic strength of the solution,  $I$ , is defined as

$$I = \frac{1}{2} \sum_j |z_j| z_j^2 \quad (24)$$

where  $z_j$  is the charge number of the ion. The binary interaction parameters,  $\beta_{ij}$ , in eq 21 cannot be computed theoretically, and therefore, the values of these parameters need to be obtained by fitting the model to the experimental VLE data. For the present amino acid salt–CO<sub>2</sub> system comprising nine solute species in the liquid phase, the number of possible binary interactions is too large for a meaningful estimation to be made of them all. However, the following general rules were used to reduce the number of interaction parameters and they are described in detail by Weiland et al.<sup>16</sup> (1) The interactions between ions of similar charge were neglected. (2) The interactions of all ionic and molecular species with water and its ionization products were neglected. (3) The interactions between CO<sub>2</sub> and other solute species were neglected. (4) All interactions with CO<sub>3</sub><sup>2-</sup> were neglected.

Basically, the last two assumptions are related to the very low concentrations of these species that occur in the liquid phase. By this procedure, the number of interactions (and interaction parameters,  $\beta_{ij}$ ) to be considered in the regression reduces to those between the following eight pairs of species:



The set of equations including the activity coefficient model was solved numerically using commercially available MATLAB software, in which the following objective function for minimization was used<sup>16</sup>

$$F_i = \frac{(p_{CO_2}^{\text{exp}} - p_{CO_2}^{\text{m}})^2}{p_{CO_2}^{\text{exp}} p_{CO_2}^{\text{m}}} \quad (25)$$

where the superscripts exp and m denote experiment and model, respectively.

The initial guess values for the concentrations of the nine solute species in the liquid phase were obtained by setting all interaction parameters in eq 21 equal to 0 (the model then reduces to the Debye–Hückel expression). The equilibrium constants in eqs 9–12 were obtained from the literature and are shown in Table 1.

In addition, the value used for the carbamate hydrolysis equilibrium constant,  $K_{\text{carb}}$  (eq 8), was that determined experimentally in the present work (see section 4.1). Already at this stage, the calculated values of  $P_{CO_2}$  were reasonably accurate. Some “bad” data points in the experimental data set (data for a single amino acid salt concentration) were eliminated using the methodology described in detail by Weiland et al.<sup>16</sup> This procedure involves the elimination of any data point for which the predicted vapor pressure of CO<sub>2</sub> deviates from the experimental value by more than a factor 2 from the data set. This approach avoided problems in the convergence of the fitting procedure in the subsequent step when the binary interaction parameters were taken into account in the expression for the activity coefficient. However, the present experimental data were obtained in a relatively narrow range of partial pressures of CO<sub>2</sub> (compared to the variation of 5–6 orders studied by Weiland et al.<sup>16</sup>), and hence, the number of bad data points was insignificant. In the second step, the binary interaction parameters ( $\beta_{ij}$ ) as well as the equilibrium constants  $K_{\text{carb}}$  (depending on the availability of the experimental values) were used as fit parameters in the model, and the experimental data were regressed with the complete model to determine the above constants.

### 3. Experimental Section

**3.1. Chemicals.** The potassium salt solution of tau-rine was prepared by neutralizing the amino acid (Merck) dissolved in deionized water, with a slightly less than equimolar (known) quantity of potassium hydroxide (Merck) in a standard flask. The remaining amount of KOH was added precisely by potentiometrically titrating the solution with an aqueous KOH solution of known strength. The concentration of the aqueous amino acid salt (or deprotonated amino acid) solution prepared was cross-checked by titrating it with standard HCl solutions.

**3.2. Experimental Setup and Procedure.** The schematic diagram of the experimental setup is shown in Figure 1. The principle part of the setup was a double-walled (glass) reactor of approximately 1600 cm<sup>3</sup> volume. The reactor was provided with a high-intensity gas-inducing stirrer in the liquid phase and a propeller-type impeller in the gas phase. Also, the reactor was equipped with a digital pressure transducer, a thermocouple, and a pH electrode. A continuous dilute CO<sub>2</sub> gas stream of known composition was prepared by mixing flows of pure CO<sub>2</sub> and N<sub>2</sub> at desired flow rates using mass flow controllers. Two double-walled (glass) water-vapor saturators were used to saturate the N<sub>2</sub> and CO<sub>2</sub> gas streams separately before they were mixed to prepare the feed gas. Whereas the nitrogen stream was saturated with an amino acid salt solution identical to that used in the reactor, the CO<sub>2</sub> stream was saturated with water. The gas stream was fed to the reactor using a sintered stainless steel sparger located below the impeller of the liquid phase. The outlet gas stream from the reactor was led to a cold trap to condense all of the water vapor, and the concentration of CO<sub>2</sub> in the gas stream from the cold trap was subsequently analyzed using an infrared CO<sub>2</sub> analyzer. Before the experiment, the feed gas stream was passed through a two-way valve that was used to bypass the reactor to determine the concentration of CO<sub>2</sub> in the feed gas. The contents of the stirred reactor and vapor saturators were maintained at a constant temperature using a thermostatic

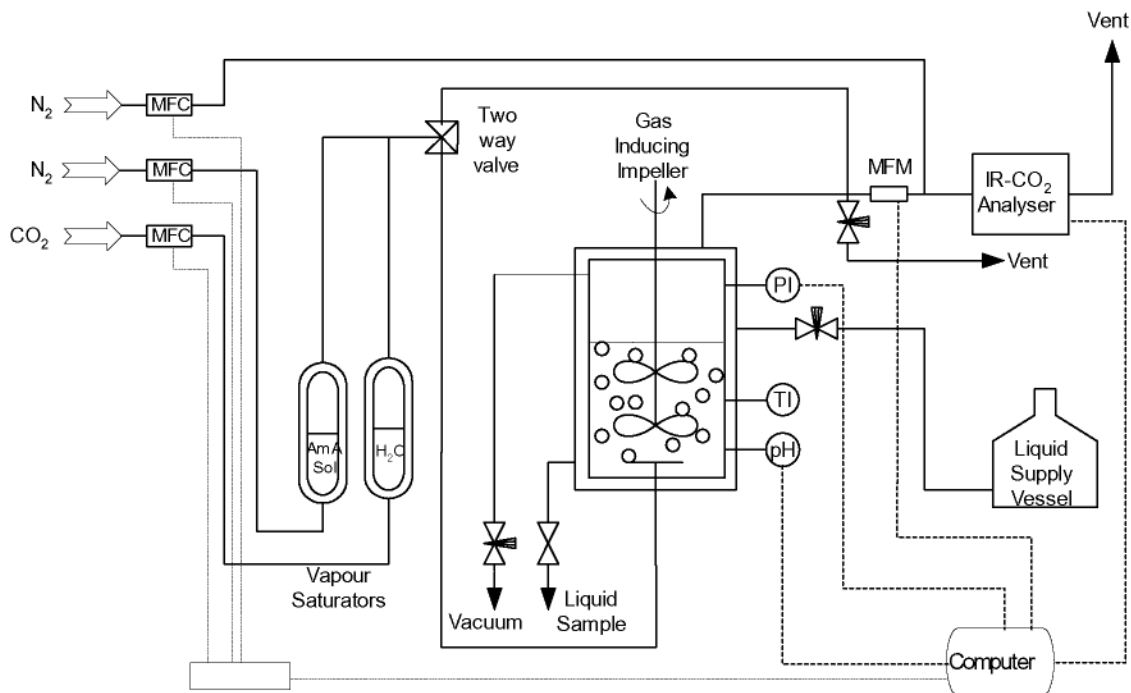


**Figure 1.** Schematic diagram of the experimental setup.

water bath. The measurements of all of the instruments were recorded by a computer using a data acquisition system.

In a typical experimental run, a known volume ( $\sim 500$  mL) of the amino acid salt solution was charged into the reactor. It was stirred for 30 min to reach the desired absorption temperature. The mass flow controllers were adjusted to obtain the desired flow rates of  $N_2$  and  $CO_2$ . The concentration of  $CO_2$  in the feed gas stream was measured in the gas analyzer by bypassing the stirred reactor (using the two-way valve). Subsequently, the gas stream was allowed to flow through the reactor, and the outlet gas stream  $CO_2$  concentration was monitored in the IR gas analyzer. Equilibrium was attained when the outlet and feed gas stream  $CO_2$  concentration were the same. Because dilute ( $< 6.0$  vol %  $CO_2$ ) gas streams were used for absorption, very long times were generally required to reach equilibrium. Therefore, a known amount of pure  $CO_2$  from a calibrated gas supply vessel was used to preload the amino acid salt solution before the above-described equilibrium experiments. This considerably reduced the experimental time. Because several (maximum of four to five) experiments were conducted in succession with the same solution (stepwise loading), the concentration of the amine in the reactor was checked by titration as described previously. The change in the amino acid salt concentration during one set of experiments (consisting of a maximum of four to five experiments) was within 2.5%. After equilibrium between the gas and liquid phase was attained in the reactor, a liquid sample of known volume was collected in a known volume of standard alkali (NaOH) solution. The pH of the loaded solution in the reactor was measured at the time of sampling. The sample was subsequently analyzed for  $CO_2$  loading using an analytical method similar to the one described in detail by Blauwhoff et al.<sup>21</sup> All experiments were conducted at near-atmospheric pressure in the reactor and for two absorption temperatures, namely, 298 and 313 K. Crystallization was observed in the loaded solutions for

potassium taurate concentrations of  $2000 \text{ mol m}^{-3}$  and above. In these situations, the clear, solid-free liquid present in the reactor was used for determining the liquid  $CO_2$  loading.

**3.3. Carbamate Hydrolysis.** The carbamate hydrolysis equilibrium constant ( $K_{\text{carb}}$  in eq 8) for the potassium salt of taurine was independently measured using an experimental technique identical to the one reported by Chan and Danckwerts.<sup>22</sup> A reaction mixture containing equimolar quantities of amine and potassium bicarbonate was prepared in a reaction flask and was allowed to equilibrate for 24 h in a thermostatic shaker at 298 K. After equilibration, the bicarbonate in the solution was precipitated as  $BaCO_3$  by the addition of excess alkaline  $BaCl_2$ . The reaction mixture was immediately filtered and washed with a known amount of deionized water. The filtrate was quickly titrated with a standard HCl solution. From the amount of HCl consumed in the titration, the carbamate hydrolysis equilibrium constant,  $K_{\text{carb}}$ , was calculated using the procedure described in detail by Chan and Danckwerts.<sup>22</sup> The precipitation of the bicarbonate and subsequent filtration was done very fast to avoid a change in the equilibrium composition of the reaction mixture resulting from the removal of  $HCO_3^-$ . Therefore, only very low concentrations of the amino acid salt and bicarbonate ( $< 300 \text{ mol m}^{-3}$ ) were used in the reaction mixture. The experimental technique was initially standardized for monoethanolamine, for which a limited number of experimental data on  $K_{\text{carb}}$  are available in the literature. The influence of the ionic strength on the carbamate hydrolysis constant of monoethanolamine was studied at 298 K by performing the above experiments in the presence of a known amount of an inert and strong electrolyte (KCl). For MEA, the experiments were conducted for two initially equimolar concentrations of the amine and bicarbonate in the reaction mixture, namely, 100 and  $200 \text{ mol m}^{-3}$ .

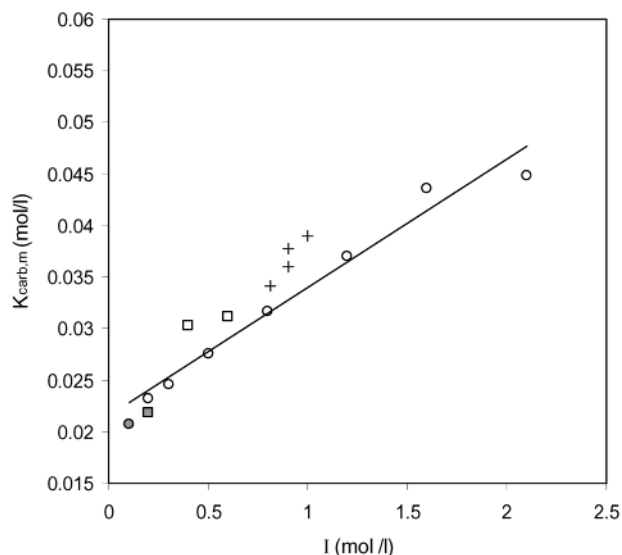


**Figure 2.** Influence of the ionic strength on the carbamate hydrolysis equilibrium constant of MEA at 298 K (+, Danckwerts and Chan;<sup>22</sup> O, present work with  $[\text{MEA}]_0 = [\text{HCO}_3^-]_0 = 100 \text{ mol m}^{-3}$ ; □, present work with  $[\text{MEA}]_0 = [\text{HCO}_3^-]_0 = 200 \text{ mol m}^{-3}$ ). The dark points in the figure indicate the measurements done without KCl in the reaction mixture.

**Table 2. Carbamate Hydrolysis Equilibrium Constants of Aqueous Potassium Taurate at 298 K**

$[\text{RNH}_2]_0$ ( $\text{mol m}^{-3}$ ) $\times 10^{-3}$	$[\text{HCO}_3^-]_0$ ( $\text{mol m}^{-3}$ ) $\times 10^{-3}$	$K_{\text{carb,m}}$ ( $\text{mol m}^{-3}$ ) $\times 10^{-3}$
0.10	0.10	0.0531
0.15	0.15	0.0532
0.20	0.20	0.0482
0.30	0.30	0.0509

## 4. Results and Discussion

**4.1. Carbamate Hydrolysis Equilibrium Constant ( $K_{\text{carb}}$ ).**  $K_{\text{carb}}$  is one of the constants in the above-described equilibrium model that is usually obtained by fitting the VLE model to the experimental equilibrium  $\text{CO}_2$  solubility data. If  $K_{\text{carb}}$  can be estimated independently for the experimental conditions of interest in the actual gas-treating processes (data at high ionic strength of the solution), the number of fit parameters in the VLE model can be reduced. In this way, the simple Kent–Eisenberg equilibrium model for the primary and secondary amines can be used to quantitatively describe the vapor–liquid equilibria of a given  $\text{CO}_2$ –amine system without any fit parameters. Information on the values of the other equilibrium constants, such as  $K_{\text{AmA}}$  and  $K_{\text{CO}_2}$ , can be obtained from the literature at different temperatures (see Table 1). In general, the sensitivity of the predicted  $\text{CO}_2$  vapor pressure to the carbamate hydrolysis constant is at its maximum for liquid  $\text{CO}_2$  loadings between 0.1 and 0.4 mol of  $\text{CO}_2$  per mole of amino acid salt.

It has been shown for primary and secondary alkanolamines (but only with limited experimental data) that  $K_{\text{carb}}$  has a more or less strong dependence on the ionic strength of the solution.<sup>22</sup> Information on the stability of the carbamates of amino acids (inversely proportional to  $K_{\text{carb}}$ ) is scarce and very old, with no published data on  $K_{\text{carb}}$  for taurine.

To begin, the influence of the ionic strength of the solution on  $K_{\text{carb}}$  was studied for monoethanolamine at 298 K, as only a limited amount of experimental data for solutions of low ionic strength is available in the

literature. Two different initial equimolar concentrations of amine and bicarbonate in the reaction mixture were used, along with different concentrations of KCl. The results for  $K_{\text{carb}}$  are shown in Figure 2 as a function of the ionic strength of the reaction mixture. The constant  $K_{\text{carb,m}}$  shown in the figure is based on molar concentration units and is defined as

$$K_{\text{carb,m}} = \frac{[\text{RNH}_2]_{\text{m}}[\text{HCO}_3^-]_{\text{m}}}{[\text{RHNCOO}]_{\text{m}}} \quad (26)$$

where the subscript m indicates that the concentrations are expressed in molar units.

The experimental results of Chan and Danckwerts<sup>22</sup> are also shown in Figure 2. It should be noted that these authors also used  $\text{Na}_2\text{CO}_3$  along with the amine and bicarbonate in the initial reaction mixture. Although the range of amine and bicarbonate concentrations studied in the present work (with no KCl in the reaction mixture) is comparable to that used by Chan and Danckwerts, the ionic strengths of the solutions in their experiments were higher because of the presence of carbonate. The results shown in the Figure 2 indicate that  $K_{\text{carb}}$  is strongly influenced by the ionic strength of the solution, and the results of Chan and Danckwerts fall in line with the present experimental results. For MEA solutions with high ionic strength such as usually encountered in industrial applications, the value of  $K_{\text{carb}}$  could differ significantly from the experimental values reported for low ionic strengths. A linear regression of the experimental data obtained from the present work gave the following expression

$$K_{\text{carb,m}} = 0.0124I + 0.0216 \quad (27)$$

Using the above experimental procedure, the carbamate hydrolysis equilibrium constant of the potassium salt of taurine was also measured at 298 K, and the results are shown in Table 2. From these results, it is clear that the carbamate of taurine is reasonably stable (comparable in stability to the carbamates of primary amines), but somewhat less stable than the carbamate of MEA. Although the variation in the experimental initial concentrations of the amino acid salt and bicarbonate was limited, there does not seem to be a significant influence of the ionic strength of the solution on the equilibrium constant. However, the range of experimental data is rather limited for definitive conclusions to be made. In Table 3,  $K_{\text{carb,m}}$  values for some similar amino acids (with a single primary amino functional group) reported in the literature<sup>23</sup> are given. The experimental measurements were done for very low amino acid concentrations, as in the present study. The values reported by Rochelle et al.<sup>23</sup> for 298 K were estimated (using information on the heat of reaction of the carbamate hydrolysis reaction,  $-\Delta H_{\text{R}}$ ) from the original data, which were measured at 291 K. There does not seem to be any clear trend between  $K_{\text{carb,m}}$  and the basicity of the amine ( $\text{p}K_{\text{a}}$ ). Nevertheless, the stabilities of the carbamates of all amino acids, except  $\alpha$ -alanine, are comparable to those of primary alkanolamines. It is a well-established theory that substitution at the  $\alpha$ -carbon atom adjacent to the amino group of an amine reduces the stability of the carbamate, resulting in enhanced hydrolysis of the carbamate to bicarbonate/carbonate.<sup>24</sup> This could explain the relative instability (or high  $K_{\text{carb,m}}$  value) of the carbamate of  $\alpha$ -alanine.

**Table 3. Carbamate Hydrolysis Constants for Various Amino Acids Reported in the Literature (Rochelle et al.<sup>23</sup>)**

amino acid	$K_{\text{carb,m}}$ at 291 K (mol m <sup>-3</sup> ) × 10 <sup>-3</sup>	$K_{\text{carb,m}}$ at 298 K (mol m <sup>-3</sup> ) × 10 <sup>-3</sup>	p <i>K</i> <sub>a</sub> at 298 K	original source of data for $K_{\text{carb,m}}$ at 291 K
glycine (H <sub>2</sub> NCH <sub>2</sub> CO <sub>2</sub> H)	0.033	0.042	9.78	Jensen et al. <sup>25</sup>
α-alanine (CH <sub>3</sub> CH(NH <sub>2</sub> )CO <sub>2</sub> H)	0.108	0.125	9.87	Jensen and Faurholt <sup>8</sup>
β-alanine (H <sub>2</sub> NCH <sub>2</sub> CH <sub>2</sub> COOH)	0.031	0.039	10.41	Jensen and Faurholt <sup>8</sup>
taurine (H <sub>2</sub> NCH <sub>2</sub> CH <sub>2</sub> SO <sub>3</sub> H)	—	0.051	9.08	present work

**Table 4. Solubility of CO<sub>2</sub> in Aqueous Potassium Taurate Solutions at 298 and 313 K**

<i>T</i> = 298 K			
$\alpha$ (mol of CO <sub>2</sub> ) (mol of AmA)	<i>P</i> <sub>CO<sub>2</sub></sub> (kPa)	$\alpha$ (mol of CO <sub>2</sub> ) (mol of AmA)	<i>P</i> <sub>CO<sub>2</sub></sub> (kPa)
[−RNH <sub>2</sub> ] <sub>0</sub> = 500 mol m <sup>-3</sup>		[−RNH <sub>2</sub> ] <sub>0</sub> = 1000 mol m <sup>-3</sup>	
0.396	0.203	0.366	0.202
0.405	0.204	0.376	0.201
0.444	0.318	0.403	0.314
0.486	0.598	0.437	0.456
0.532	0.892	0.486	0.811
0.541	1.003	0.509	1.297
0.569	2.087	0.532	1.824
0.586	2.999	0.550	2.847
0.592	4.083	0.565	4.701
0.608	5.117	0.567	3.951
0.614	5.887	0.577	5.623
[−RNH <sub>2</sub> ] <sub>0</sub> = 2000 mol m <sup>-3</sup>		[−RNH <sub>2</sub> ] <sub>0</sub> = 3000 mol m <sup>-3</sup>	
0.353	0.221	0.360	0.107 <sup>a</sup>
0.385	0.318	0.391	0.147 <sup>a</sup>
0.400	0.401	0.449	0.252 <sup>a</sup>
0.433	0.658	0.520	1.058 <sup>a</sup>
0.466	1.232	0.547	1.950 <sup>a</sup>
0.464	1.054		
0.483	1.560		
0.497	2.938	[−RNH <sub>2</sub> ] <sub>0</sub> = 4000 mol m <sup>-3</sup>	0.394
0.524	4.336 <sup>a</sup>		0.429
0.525	5.198 <sup>a</sup>		0.449
0.549	6.008 <sup>a</sup>		0.476
0.583	5.978 <sup>a</sup>		0.487
0.602	6.586 <sup>a</sup>		
0.622	7.396 <sup>a</sup>		

*T* = 313 K

$\alpha$ (mol of CO <sub>2</sub> ) (mol of AmA)	<i>P</i> <sub>CO<sub>2</sub></sub> (kPa)
[−RNH <sub>2</sub> ] <sub>0</sub> = 1000 mol m <sup>-3</sup>	
0.225	0.280
0.276	0.546
0.317	0.886
0.351	1.483
0.355	1.489
0.410	3.063
0.435	3.639
0.461	4.488
0.475	5.286

<sup>a</sup> For these experimental conditions, crystallization was observed in the stirred reactor.

**4.2. CO<sub>2</sub>—Aqueous Potassium Taurate Vapor—Liquid Equilibria.** Table 4 contains the experimental CO<sub>2</sub> solubility data measured at 298 and 313 K. The experimental measurements were conducted in the range of partial pressures of CO<sub>2</sub> varying between 0.1 and 6.0 kPa, which is the range typically encountered in the removal of CO<sub>2</sub> from flue gas. The experimental VLE data obtained from the present study, as shown in Figure 3, indicate that the equilibrium absorption capacity of CO<sub>2</sub> in aqueous potassium taurate solutions

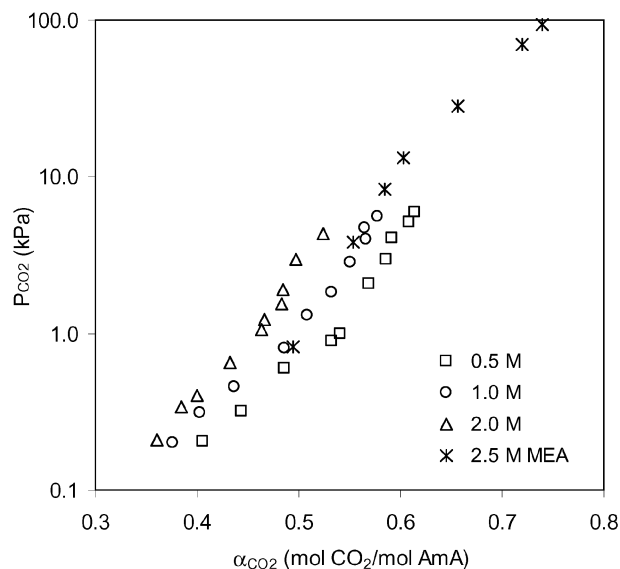


**Figure 3.** Equilibrium solubility of CO<sub>2</sub> in aqueous potassium taurate solutions at 298 K. Also shown is the solubility of CO<sub>2</sub> in 2.5 M aqueous monoethanolamine solutions at 298 K.<sup>26</sup> The legend of the figure indicates the total molar amine concentration ([−RNH<sub>2</sub>]<sub>0</sub>).

for a given *P*<sub>CO<sub>2</sub></sub> seems to be comparable to that of primary alkanolamines (say, monoethanolamine) of similar concentration. The lower *P*<sub>CO<sub>2</sub></sub> over the MEA solution can possibly be explained in terms of the basicity (p*K*<sub>a</sub>) of the amines.

Neglecting α-alanine (for which the amino group is attached to the α-carbon atom, a feature known to affect the stability of the carbamates) in Table 3, it can be reasonably concluded that the stabilities of the carbamates increase with increasing basicity (p*K*<sub>a</sub>) of the amino acid. Extrapolating the above observation to MEA, which is more basic (p*K*<sub>a</sub> = 9.54) than taurine, one can expect the carbamate of MEA to be more stable than that of taurine. This can also be observed from the experimental values of the carbamate hydrolysis constants for MEA (see Figure 2). The overall amine—CO<sub>2</sub> VLE can be simplistically represented using eq 13. With an increase in p*K*<sub>a</sub> of the amine, *K*<sub>AmA</sub> and *K*<sub>carb</sub> should decrease, and consequently, *K*<sub>ov</sub> should increase. This indicates that the concentration of CO<sub>2</sub> in the liquid phase (or *P*<sub>CO<sub>2</sub></sub>) should decrease. Therefore, for MEA, the equilibrium value of *P*<sub>CO<sub>2</sub></sub> for a given acid gas loading can be expected to be lower than that of a corresponding aqueous potassium taurate solution. However, only a limited amount of experimental data is available in the literature for MEA at 298 K, especially for amine concentrations of less than 2500 mol m<sup>-3</sup>, and it is difficult to arrive unambiguously at the above conclusion from experimental observations alone.

As mentioned earlier, crystallization was observed in the higher range of *P*<sub>CO<sub>2</sub></sub> values for solutions with high

amino acid salt concentrations (2 M and above). However, the initial analysis and discussion of the experimental VLE data will be focused on situations where no crystallization occurred; cases involving crystallization will be considered subsequently in section 4.3. The experimental data were regressed with the VLE model to obtain the binary interaction parameters in the extended Debye–Hückel expression, as well as  $K_{\text{carb}}$ . The experimental values of  $K_{\text{carb}}$  obtained in the present study are valid only for solutions of low ionic strengths, and therefore,  $K_{\text{carb}}$  was also used as a fit parameter in the data regression (to study the influence of the amino acid salt concentration or ionic strength on  $K_{\text{carb}}$ ). As mentioned in section 2.3, in the initial regression of the experimental data, the  $\beta_{ij}$ 's were set to zero, and only  $K_{\text{carb}}$  was used as a fitting parameter. Analysis of the calculated equilibrium concentrations of the nine species in the liquid phase (as predicted by the model) indicated that the change in the ionic strength of the solution for the range of  $\alpha_{\text{CO}_2}$  values studied in the present work varied between 3 and 6% for different amino acid salt concentrations (see also Figure 4). In such a situation, the first term (Debye–Hückel) in the extended Debye–Hückel expression becomes essentially constant. This means that eq 21 basically reduces to

$$\ln \gamma_i = C + 2 \sum_{j \neq w} \beta_{ij} |j| \quad (28)$$

Such remarkable behavior can be understood from arguments based on the asymptotic situations in the absorption of  $\text{CO}_2$  in aqueous alkaline salt solutions of amino acids and alkanolamines. In the following discussion, the subscript AmA and AA refer to the amino acid salt and alkanolamine, respectively.

(1) Unlike aqueous alkanolamines (for which the ionic strength is near zero for unloaded solutions), the ionic strength of unloaded aqueous amino acid salt solutions is the molal salt concentration

$$\text{For } \alpha_{\text{CO}_2} = 0, \quad I_{\text{AmA}} = [\text{RNH}_2]_0 \\ I_{\text{AA}} \approx 0$$

(2) For the asymptotic situation of complete conversion of the amine but negligible hydrolysis of the carbamate, as described by reaction 2, the  $\text{CO}_2$  loading of the solution is 0.5 mol of  $\text{CO}_2$  per mole of amino acid salt. Then, the ionic strengths of the aqueous amino acid salt and alkanolamine solutions are

$$\text{For } \alpha_{\text{CO}_2} = 0.5, \\ I_{\text{AmA}} = \frac{1}{2} \{ [\text{RNHCOO}^-](-2)^2 + [\text{RNH}_3^+](0)^2 + [\text{K}^+](1)^2 \} \\ = \frac{1}{2} \{ 0.5[\text{RNH}_2]_0(-2)^2 + 0.5[\text{RNH}_2]_0(0)^2 + [\text{RNH}_2]_0(1)^2 \} \\ = 1.5[\text{RNH}_2]_0 \\ I_{\text{AA}} = \frac{1}{2} \{ [\text{RNHCOO}^-](-1)^2 + [\text{RNH}_3^+](1)^2 \} \\ = 1.0[\text{RNH}_2]_0$$

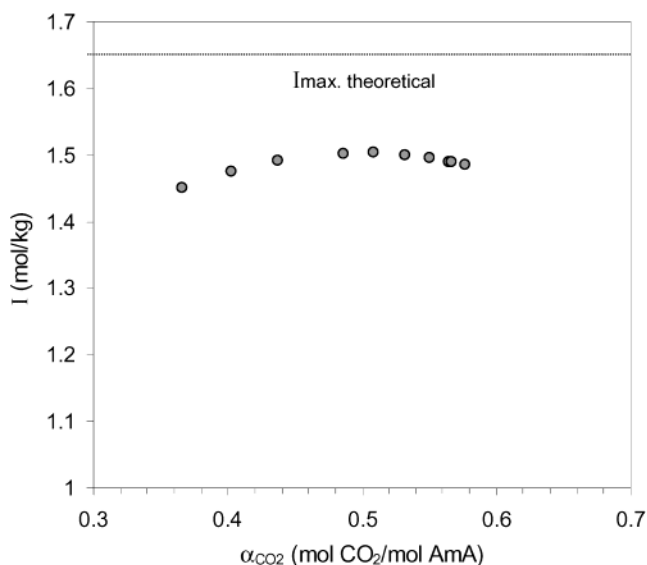
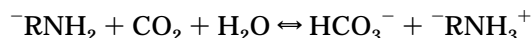


**Figure 4.** Influence of  $\text{CO}_2$  absorption on the ionic strength of 1.0 M ( $\sim 1.1$  m) aqueous potassium taurate solution at 298 K. Ionic strength calculated on the basis of the results obtained with the Debye–Hückel model.

(3) Assuming complete hydrolysis of the carbamate, the absorption capacity of the amine solutions can reach the theoretical maximum of 1.0 mol of  $\text{CO}_2$  per mole of amine as per the following overall reaction for amino acids



For  $\alpha_{\text{CO}_2} = 1.0$ ,

$$I_{\text{AmA}} = \frac{1}{2} \{ [\text{HCO}_3^-](-1)^2 + [\text{RNH}_3^+](0)^2 + [\text{K}^+](1)^2 \} \\ = 1.0[\text{RNH}_2]_0 \\ I_{\text{AA}} = \frac{1}{2} \{ [\text{HCO}_3^-](-1)^2 + [\text{RNH}_3^+](1)^2 \} \\ = 1.0[\text{RNH}_2]_0$$

Therefore, during the absorption of  $\text{CO}_2$  in aqueous amino acid salt solutions, the ionic strength changes from the initial amino acid salt concentration ( $[\text{RNH}_2]_0$ ) to the maximum possible value ( $I_{\text{max}}$ ) of  $1.5[\text{RNH}_2]_0$  corresponding to asymptotic case 2. For  $\text{CO}_2$  loadings larger than 0.5 mol of  $\text{CO}_2$  per mole of amino acid salt, the ionic strength decreases with increasing  $\alpha_{\text{CO}_2}$  and eventually reaches the value of an unloaded solution. In reality, the carbamate hydrolysis becomes significant even at  $\alpha_{\text{CO}_2}$  values as low as 0.1, and therefore, the actual maximum value is less than the theoretical maximum value ( $1.5[\text{RNH}_2]_0$ ; see also Figure 4). This behavior is very different from that of aqueous alkanolamines. Figure 4 shows the ionic strength of a 1.0 M aqueous potassium taurate solution as a function of  $\text{CO}_2$  loading. The ionic strength of the solution given in the figure was calculated from the individual species concentrations predicted by the VLE model neglecting the interaction parameters ( $\beta_{ij}$ ).

This indeed shows that the extended Debye–Hückel expression (eq 21) essentially reduces to eq 28 for the experimental data obtained in the present work. However, eq 28 loses the thermodynamic soundness of the

**Table 5. Fitted Equilibrium Constants for Different Data Sets**

$T$ (K)	$[-\text{RNH}_2]_0$ (mol m <sup>-3</sup> )	$K_{\text{AmA}}^{\text{m}}$ (mol kg <sup>-1</sup> )	$K_{\text{carb}}^{\text{m}}$ (mol kg <sup>-1</sup> )	$K_{\text{AmA,m}}^{\text{m}}$ (mol m <sup>-3</sup> ) × 10 <sup>-3</sup>	$K_{\text{carb,m}}^{\text{m}}$ (mol m <sup>-3</sup> ) × 10 <sup>-3</sup>	$K_{\text{AmA,m, lit}}^{\text{a}}$ (mol m <sup>-3</sup> ) × 10 <sup>-3</sup>
298	500	$4.40 \times 10^{-10}$	0.021	$1.27 \times 10^{-9}$	0.019	$8.91 \times 10^{-10}$
298	1000	$4.39 \times 10^{-10}$	0.053	$1.18 \times 10^{-9}$	0.048	$8.91 \times 10^{-10}$
298	2000	$3.74 \times 10^{-10}$	0.105	$9.05 \times 10^{-10}$	0.085	$8.91 \times 10^{-10}$
313	1000	$1.15 \times 10^{-10}$	0.937	$3.07 \times 10^{-9}$	0.847	$1.94 \times 10^{-9}$

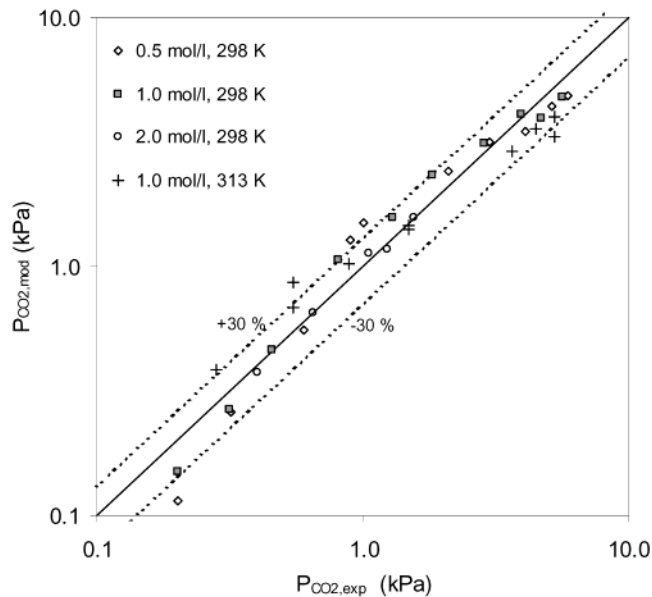
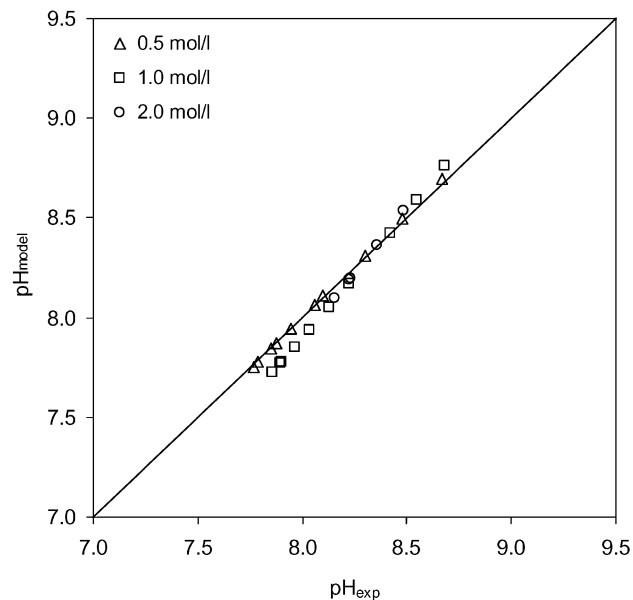
<sup>a</sup> From Perrin.<sup>7</sup>

extended Debye–Hückel expression and simply becomes an empirical fitting equation, in which the activity coefficients are related to the molal concentrations of various species in the liquid phase along with a number of associated constants. Now, the choice of the interaction parameters among the seven  $\beta$ 's mentioned in section 2.3 becomes rather empirical. Considering the above facts, it was decided to regress the experimental data with a VLE model neglecting the binary interaction parameters in the extended Debye–Hückel expression (eq 21). Because the ionic strength does not change significantly for the present experimental data, this simplification makes the model similar to the Kent–Eisenberg model, as the activity coefficient can now be calculated explicitly. As for the Kent–Eisenberg model, the amine deprotonation equilibrium constant ( $K_{\text{AmA}}$ ) was also made an adjustable fit parameter, given that the experimental data available in the literature are rather old<sup>7</sup> and information about its accuracy is not known. Thus, the final form of the VLE model used contained two fitting parameters, namely,  $K_{\text{carb}}$  and  $K_{\text{AmA}}$ . Table 5 shows the optimal values of the fitting parameters obtained in the regressions for different experimental data sets.

The values of  $K_{\text{carb}}^{\text{m}}$  and  $K_{\text{AmA}}^{\text{m}}$  given in Table 5 are the apparent equilibrium constants (in molal units) obtained by lumping the activity coefficients of the species involved in the reactions (and the activity of water,  $a_{\text{w}}$ , in the case of  $K_{\text{carb}}^{\text{m}}$ ) with  $K_{\text{carb}}$  and  $K_{\text{AmA}}$ , respectively. The amine dissociation constant,  $K_{\text{AmA}}$ , is within 35% of the experimental value reported in the literature. The carbamate hydrolysis constant shows a strong dependence on the initial amino acid salt concentration (or ionic strength of the solution). However, such a trend could not be clearly observed from the measured  $K_{\text{carb}}$  data, which are limited in number and range (see Table 2). In fact, the observed dependence of  $K_{\text{carb}}^{\text{m}}$  on the ionic strength seems to be much larger than that for MEA, for which the experimental values are reported as a function of the ionic strength of the solution in section 4.1.

Finally, the most important aspect of a VLE model is the accuracy of its predictions of the experimental data. Figure 5 shows the parity plot for the experimental and predicted values of the partial pressure of CO<sub>2</sub>. The average error in the prediction of  $P_{\text{CO}_2}$  is 16.5%. Figure 6 shows the parity plot of the predicted and experimentally determined values of the pH's of the loaded potassium taurate solutions at 298 K. The average error in the prediction of the solution pH is 0.54%.

**4.3. Crystallization in Aqueous Potassium Taurate Solutions and Its Influence on the Vapor–Liquid Equilibria.** Hook<sup>3</sup> reported that the products of the reaction between CO<sub>2</sub> and certain aqueous alkaline salts of amino acids (say, alanine), and especially C<sub>α</sub>-substituted amino acids (such as 2-methylglycine), undergo crystallization at moderate to high conversions of the amino acid salt. In a recent study,

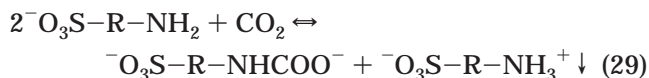
**Figure 5.** Parity plot of predicted and experimental values of the vapor pressure of CO<sub>2</sub> above aqueous potassium taurate solutions at 298 and 313 K.**Figure 6.** Parity plot of predicted and experimental values of the pH of CO<sub>2</sub>-loaded aqueous potassium taurate solutions (corresponding to the solubility data at 298 K). The legend of the figure indicates the total molar amino acid salt concentration ( $[-\text{RNH}_2]_0$ ).

Kumar et al.<sup>4</sup> reported crystallization during the absorption of CO<sub>2</sub> in aqueous potassium taurate solutions as well. Following are some important conclusions made from that investigation:

(1) For aqueous potassium taurate solutions, crystallization of the reaction product occurs even at moderate CO<sub>2</sub> loadings (0.20–0.5 mol of CO<sub>2</sub> per mole of AmA),

depending on the total amino acid salt concentration ( $[\text{RNH}_2]_0$ ).

(2) The crystallizing reaction product is the protonated amine (or zwitterionic form of the amino acid).



(3) There is a clear relationship between the critical  $\text{CO}_2$  loading value ( $\alpha_{\text{CO}_2, \text{crit}}$ ) at which crystallization of the reaction product occurs and the solubility of the zwitterionic form of taurine.

$$\alpha_{\text{CO}_2, \text{crit}} = \frac{S}{[\text{RNH}_2]_0} \quad (30)$$

Here,  $S$  is the solubility of the amino acid in the solution, and  $[\text{RNH}_2]_0$  is the total amino acid salt concentration. The inverse relationship between  $\alpha_{\text{CO}_2, \text{crit}}$  and  $[\text{RNH}_2]_0$  indicates that the crystallization will occur much earlier (in terms of  $\text{CO}_2$  loading) for higher amino acid salt concentrations.

(4) The formation of crystals in the liquid phase appears (semiquantitatively) to reduce the volumetric mass-transfer coefficient ( $k_{l,a}$ ) of the gas-liquid contactor.

The results presented in this section are related to another important aspect of the crystallization phenomenon that was not addressed in the earlier work, i.e., the influence of the crystallization of the reaction product on the vapor-liquid equilibrium of the  $\text{CO}_2$ -aqueous potassium taurate system. For equilibrium-limited liquid-phase reactions, the selective removal of a reaction product from the reaction mixture will essentially shift the equilibrium toward the product side.<sup>27</sup> This technique is widely used in industry to enhance the equilibrium conversion of reversible reactions. For the present  $\text{CO}_2$ -amino acid salt system as well, crystallization of the reaction product (protonated amine) can be expected to increase the  $\text{CO}_2$  absorption capacity of the aqueous amino acid salt solutions for a given partial pressure of  $\text{CO}_2$  in the gas phase. Therefore, this phenomenon was also investigated in the present work.

Figure 7 shows the experimental  $\text{CO}_2$  solubility data for concentrated aqueous potassium taurate solutions ( $\geq 2$  M). For 2 M solutions, crystallization was observed halfway through the range of partial pressures studied in the present work. The remarkable influence of crystallization on the equilibrium  $\text{CO}_2$  absorption capacity of the salt solution can be clearly observed from the dramatic decrease in the slope of the experimental data. However, for 3 and 4 M solutions, crystallization was observed even for partial pressures of  $\text{CO}_2$  as low as 0.1 kPa. This was expected because the critical  $\text{CO}_2$  loading values ( $\alpha_{\text{crit}, \text{CO}_2}$ ) measured in an earlier work<sup>4</sup> were approximately 0.30 and 0.17 mol of  $\text{CO}_2$  per mole of amino acid salt for 3 and 4 M salt solutions, respectively. The equilibrium partial pressures of  $\text{CO}_2$  ( $P_{\text{CO}_2}$ ) for the 3 and 4 M salt solutions (and for a given value of  $\text{CO}_2$  loading) are less than that for a 2 M amino acid salt solution. To understand the magnitude of the influence of crystallization on the  $\text{CO}_2$  absorption capacity of 3 and 4 M potassium taurate solutions, the VLE model developed earlier was used to predict the hypothetical partial pressure of  $\text{CO}_2$  for a 3 M aqueous potassium taurate solution assuming that no crystallization oc-

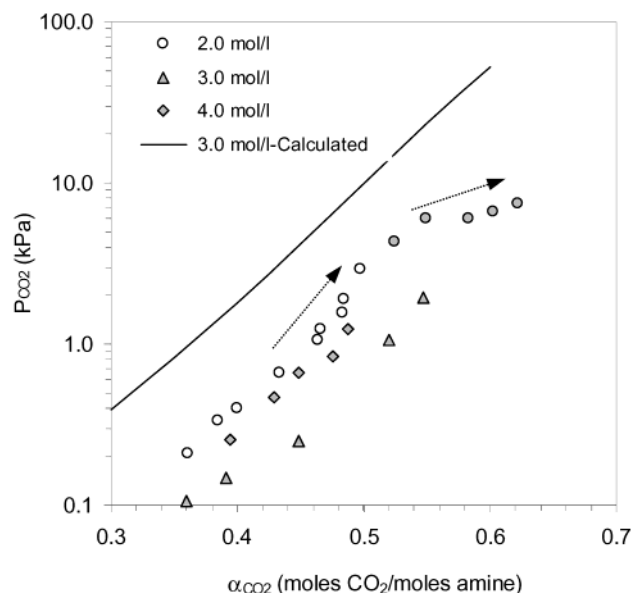


**Figure 7.** Influence of crystallization of the reaction product on the solubility of  $\text{CO}_2$  in concentrated aqueous potassium taurate solutions. The dark points in the figure indicate the presence of solids in the liquid phase at equilibrium. The continuous line in the figure indicates the hypothetical calculated partial pressure of  $\text{CO}_2$  for a 3 M solution using the VLE model and neglecting precipitation. The legend of the figure indicates the total amino acid salt concentration ( $[\text{RNH}_2]_0$ ).

curred. In the model, the value of  $K_{\text{AmA}}^{\text{m}}$  reported in Table 5 was used, whereas the  $K_{\text{carb}}^{\text{m}}$  values obtained for solutions of lower amino acid salt concentrations were linearly extrapolated. For a given value of  $\alpha_{\text{CO}_2}$ , the equilibrium vapor pressure of  $\text{CO}_2$  predicted by the model that would have occurred in the absence of crystallization is more than an order of magnitude higher than the experimental values of  $P_{\text{CO}_2}$  measured with crystallization in the loaded solution. This is a significant improvement in the capacity of the acid-gas-treating process, although it entails some negative implications associated with the handling of slurries in gas-liquid contactors. It should be noted, however, that the present equilibrium model can be extended to a situation in which the protonated amine is allowed to crystallize in the solution. In that case, the mole balance for the amine in the liquid phase (eq 18) becomes redundant, as the protonated amine ( $[\text{RNH}_3^+]$ ) crystallizes and the concentration of the protonated amine becomes equal to the solubility of the amino acid in a saturated aqueous salt solution. As the amount of reliable experimental data for conditions where crystallization occurs is limited in the present work, such a model extension is not presented here.

## 5. Conclusions

The solubility of  $\text{CO}_2$  in aqueous potassium taurate solutions was measured at 298 and 313 K for the range of  $\text{CO}_2$  partial pressure between 0.1 and 6.0 kPa. In the present work, the Deshmukh-Mather model, which is based on the extended Debye-Hückel theory, was used to describe the experimental VLE data of aqueous alkaline salt solutions of amino acids. Despite the fact that aqueous alkanolamines and amino acid salt solutions undergo similar reactions with  $\text{CO}_2$  in the liquid phase (formation of carbamate and subsequent hydrolysis of the carbamate to bicarbonate or carbonate), the

thermodynamic characteristics of the two solutions differ significantly. This is due to the difference in the ionic charges associated with the reactants and reaction products. In the range of partial pressures of CO<sub>2</sub> covered by the present experimental measurements, the change in the ionic strength of the loaded amino acid salt solution was found to be insignificant. Therefore, the Debye–Hückel term in the extended Debye–Hückel expression became essentially constant for the conditions studied, and the expression for the activity coefficient became an empirical fitting equation consisting of various interaction parameters. Consequently, the interaction parameters in the extended Debye–Hückel were neglected, and the resulting model was used to describe the experimental data. The accuracy of the predictions of the VLE model with reference to the experimental solubility data was reasonably good, and the fitting parameters, namely, the amine deprotonation constant and the carbamate hydrolysis equilibrium constant, are in agreement with the experimental values measured independently in the present study.

The equilibrium constant of the carbamate hydrolysis reaction is an important fit parameter in the VLE model. This parameter was also experimentally measured for aqueous monoethanolamine and potassium taurate solutions at 298 K. For monoethanolamine, the equilibrium constant was found to show a strong dependence on the ionic strength of the solution. For low ionic strengths, the experimental values were in good agreement with the values reported in the literature. Similarly, for potassium taurate, the experimental carbamate hydrolysis constant was found to be comparable to the data available in the literature for similar amino acids such as glycine and alanine.

During the absorption of CO<sub>2</sub> in aqueous potassium taurate solutions, crystallization of the reaction products was observed, especially for concentrated solutions. For a given partial pressure of CO<sub>2</sub> in the gas phase, crystallization was found to increase the equilibrium CO<sub>2</sub> absorption capacity of the potassium taurate solutions markedly.

## Acknowledgment

This work is part of the research program of the Centre for Separation Technology (CST), which is a collaboration between The Netherlands Organization for Applied Scientific Research (TNO) and the University of Twente. We also acknowledge H. J. Moed for the construction of the experimental setups.

## Nomenclature

$a$  = ionic size in eq 21, Å  
 $A$  = Debye–Hückel limiting slope  
 $a_w$  = activity of water, dimensionless  
 $B$  = constant in eq 21  
 $C_s$  = concentration of amino acid salt, mol m<sup>-3</sup>  
 $F_i$  = relative error of the  $i$ th measurement, dimensionless  
 $h_i$  = anion-specific constant, m<sup>3</sup> mol<sup>-1</sup>  
 $h_G$  = gas-specific constant, m<sup>3</sup> mol<sup>-1</sup>  
 $I$  = ionic strength, mol kg<sup>-1</sup>  
 $K$  = equilibrium constant, various units (but based on concentrations measured in mol/kg)  
 $K_s$  = Sechenov constant, m<sup>3</sup> mol<sup>-1</sup>  
 $m$  = physical solubility, ([CO<sub>2</sub>]<sub>liq</sub>/[CO<sub>2</sub>]<sub>gas</sub>)<sub>eq</sub>, dimensionless  
 $P$  = partial pressure, kPa  
 $P_w^{\text{sat}}$  = saturation pressure of water, kPa  
 $R$  = universal gas constant, J mol<sup>-1</sup> K<sup>-1</sup>

$S$  = solubility of the amino acid, mol kg<sup>-1</sup>

$T$  = absolute temperature, K

$z$  = valency of the ion, dimensionless

## Greek Symbols

$\alpha_{\text{CO}_2}$  = CO<sub>2</sub> loading, mol of CO<sub>2</sub>·mol of AmA<sup>-1</sup>

$\beta_{ij}$  = parameter for the interaction of species  $i$  with species  $j$ , kg mol<sup>-1</sup>

$\gamma$  = activity coefficient, dimensionless

## Subscripts

0 = initial or total

AmA = amino acid salt

carb = carbamate

m = expressed in molar units

ov = overall

w = water

## Superscripts

crit = critical, related to CO<sub>2</sub> loading

exp = experimental

m = model

## Literature Cited

- (1) Kohl, A. L.; Nielsen, R. B. *Gas Purification*; Gulf Publishing Company: Houston, TX, 1997.
- (2) Kumar, P. S.; Hogendoorn, J. A.; Feron, P. H. M.; Versteeg, G. F. New absorption liquids for the removal of CO<sub>2</sub> from dilute gas streams using membrane contactors. *Chem. Eng. Sci.* **2002**, *57* (9), 1639.
- (3) Hook, R. J. An investigation of some sterically hindered amines as potential carbon dioxide scrubbing compounds. *Ind. Eng. Chem. Res.* **1997**, *36* (5), 1779.
- (4) Kumar, P. S.; Hogendoorn, J. A.; Feron, P. H. M.; Versteeg, G. F. Equilibrium solubility of CO<sub>2</sub> in aqueous potassium taurate solutions: Part 1. Crystallization in carbon dioxide loaded aqueous salt solutions of amino acids. *Ind. Eng. Chem. Res.* **2003**, *42*, 2832–2840.
- (5) Deshmukh, R. D.; Mather, A. E. A mathematical model for equilibrium solubility of hydrogen sulfide and carbon dioxide in aqueous alkanolamine solutions. *Chem. Eng. Sci.* **1981**, *36*, 355.
- (6) Greenstein, J. P.; Winitz, M. *Chemistry of the Amino Acids*; Wiley: New York, 1961.
- (7) Perrin, D. D. *Dissociation of Organic Bases in Aqueous Solutions*; Butterworth: London, 1965.
- (8) Jensen, A.; Faurholt, C. Studies on carbamates V. The carbamates of  $\alpha$ -alanine and  $\beta$ -alanine. *Acta Chem. Scand.* **1952**, *6*, 385.
- (9) Penny, D. E.; Ritter, T. J. Kinetic study of the reaction between carbon dioxide and primary amines. *J. Chem. Soc., Faraday Trans.* **1983**, *79*, 2103.
- (10) Kumar, P. S.; Hogendoorn, J. A.; Feron, P. H. M.; Versteeg, G. F. Kinetics of the reaction of CO<sub>2</sub> with aqueous potassium salt of taurine and glycine. *AIChE J.* **2003**, *49*, 203–213.
- (11) Weisenberger, S.; Schumpe, A. Estimation of gas solubilities in salt solutions at temperatures from 273K to 363K. *AIChE J.* **1996**, *42*, 298.
- (12) Kumar, P. S.; Hogendoorn, J. A.; Feron, P. H. M.; Versteeg, G. F. Density, viscosity, solubility, and diffusivity of N<sub>2</sub>O in aqueous amino acid salt solutions. *J. Chem. Eng. Data* **2001**, *46*, 1357.
- (13) Kent, R.; Eisenberg, B. Better data for amine treating. *Hydrocarbon Process.* **1976**, *55*, 87.
- (14) Chen, C. C.; Evans, L. B. A local composition model for the excess Gibbs energy of aqueous electrolyte systems. *AIChE J.* **1986**, *32*, 444.
- (15) Austgen, D. M.; Rochelle, G. T.; Peng, X.; Chen, C. C. Model of vapor–liquid equilibria for aqueous acid gas–alkanolamine systems using the electrolyte–NRTL equation. *Ind. Eng. Chem. Res.* **1989**, *28*, 1060.
- (16) Weiland, R. H.; Chakravarty, T.; Mather, A. E. Solubility of carbon dioxide and hydrogen sulfide in aqueous alkanolamines. *Ind. Eng. Chem. Res.* **1993**, *32*, 1419.
- (17) Guggenheim, E. A. The specific thermodynamic properties of aqueous solutions of strong electrolytes. *Philos. Mag.* **1935**, *19*, 588.

(18) Butler, J. N. *Ionic Equilibrium: A Mathematical Approach*; Addison-Wesley Publishing Company: London, 1964.

(19) Tsonopolous, C.; Coulson, D. M.; Inman, L. B. Ionization constants of water pollutants. *J. Chem. Eng. Data* **1976**, *21* (2), 190.

(20) Edwards, T. J.; Maurer, G.; Newman, J.; Prausnitz, J. M. Vapor-liquid equilibrium in multicomponent aqueous solutions of volatile weak electrolytes. *AIChE J.* **1978**, *24* (6), 966.

(21) Blauwhoff, P. M. M.; Versteeg, G. F.; van Swaaij, W. P. M. A study on the reactions between CO<sub>2</sub> and alkanolamines in aqueous solutions. *Chem. Eng. Sci.* **1984**, *39* (2), 207.

(22) Chan, H. M.; Danckwerts, P. V. Equilibrium of MEA and DEA with bicarbonate and carbamate. *Chem. Eng. Sci.* **1981**, *36*, 229.

(23) Rochelle, G. T.; Bishnoi, S.; Chi, S.; Dang, H.; Santos, J. *Research Needs for CO<sub>2</sub> Capture from Flue Gas by Aqueous Absorption/Stripping*; U.S. Department of Energy Report No. DE-AF26-99FT01029; Federal Energy Technology Center: Pittsburgh, PA, 2000.

(24) Chakraborty, A. K.; Bischoff, K. B.; Astarita, G.; Damewood, J. R., Jr. Molecular orbital approach to substituent effects in amine-CO<sub>2</sub> interactions. *J. Am. Chem. Soc.* **1988**, *110* (21), 6947.

(25) Jensen, A.; Jensen, J. B.; Faurholt, C. Studies on carbamates VI. The carbamate of glycine. *Acta Chem. Scand.* **1952**, *6*, 395.

(26) Muhlbauer, H. G.; Monaghan, P. R. New equilibrium data on sweetening of natural gas with ethanolamine solutions. *Oil Gas J.* **1957**, *55* (17), 139.

(27) Westerterp, K. R.; van Swaaij, W. P. M.; Beenackers, A. A. C. M. *Chemical Reactor Design and Operation*; Wiley and Sons: New York, 1984.

*Received for review August 2, 2002*

*Revised manuscript received February 12, 2003*

*Accepted March 6, 2003*

IE020601U